Closed-Form 3-D Position Estimation Lateration Algorithm Reference Pair Selection Technique for a Multilateration System

Abdulmalik S. Yaro[1, 2], Ahmad Z. Sha'ameri[1]
[1]*Faculty of Electrical Engineering, Universiti Teknologi Malaysia, 81310 UTM, Johor Bahru, Johor, Malaysia.*
[2]*Department of Communication Engineering, Faculty of Engineering, Main Campus Ahmadu Bello University, Zaria, Nigeria.*
yaroabdulmalik@yahoo.com

***Abstract*— The position estimation (PE) accuracy of the lateration algorithm of a multilateration system depends on several factors. These factors include the number of ground receiving station (GRS)s deployed, the approach to the lateration algorithm, the geometry of the deployed GRSs, the number of GRS used as reference for the lateration algorithm and the choice of GRS used as reference to generate the time difference of arrival (TDOA) measurements for the lateration algorithm. A closed-form reference pair lateration algorithm based on a total of five GRSs is developed and a technique for selecting the suitable GRS reference pair to generate the TDOA measurements to be used with lateration algorithm is suggested. The technique is based on condition number computation and selecting the GRS pair with the least condition number as a reference for the closed-form lateration algorithm. The suggested technique is validated using 5-square and pentagon GRS configurations at some selected aircraft positions. The validation results show that the suggested technique can be used to determine the suitable GRS reference pair to generate the TDOA measurements for a passive multilateration system.**

***Index Terms*—Closed-form; Condition Number; lateration algorithm; Multilateration system; Reference selection.**

I. Introduction

Multilateration system estimates the position of an aircraft from the transponder emission detected at the antenna of the deployed ground receiving station (GRS)s. It estimates the position of the aircraft using a two-stage process [1]. The time difference of arrival (TDOA) measurements of the aircraft transponder emission detected at spatially placed GRSs are estimated at the first stage [2]. These TDOA measurements are used in the second stage with a lateration algorithm to determine the position of the aircraft. The 3-dimensional (3-D) position estimation (PE) of an aircraft requires a minimum of four GRSs [2]. The system has an advantage over multiangulation system that utilizes angle of arrival (AOA) measurements with an angulation algorithm which cannot perform 3-D PE of aircraft [3].

The TDOA measurements estimated using GRS pairs and the aircraft position have a non-linear relationship. To linearized this relationship, several approaches have been used which resulted in the two forms of lateration algorithms, namely: closed-form and open-form [4]. The open form lateration algorithm utilizes linearization algorithms such as Taylor series to obtain the linear relationship between the input variable (TDOA measurements) and output variable (aircraft position) [5–7]. This is followed by an iteration of a randomly inputted initial aircraft position while minimizing a maximum likelihood (ML) cost function. The open-form lateration algorithm is computationally complex due to the linearization and iteration processes and also suffers convergence issue [6]. In the closed-form lateration algorithm approach, an algebraic manipulation of the input and output variables is performed to obtain the linear relationship [8–14]. Unlike the open-form lateration algorithm, it always converges to a solution because there is no iteration process involved, thus, for this reason, the closed-form lateration algorithm is adopted in this work.

Compared to the open-form lateration algorithm, the closed-form lateration algorithm is sensitive to error in the input variable (TDOA estimation error) resulting to high aircraft PE error [13]. Thus, several researchers have proposed techniques to improve the PE accuracy of the lateration algorithm [9,11–15]. It was found that the PE accuracy of the lateration algorithm depends on several factors some of which are the TDOA estimation technique, the number and the geometry of the GRS deployed, the choice and number of GRSs used as reference to generate the TDOA measurements to be inputted into the lateration algorithm. To achieve a PE accuracy comparable to the surveillance radar, it is suggested that at least five GRSs be deployed for the multilateration system [2]. A TDOA residual-based method for selecting the suitable GRS to generate the TDOA measurements for use with the lateration algorithm was suggested in [12]. It assumes that an approximate position of the aircraft is known but there is a need to track the position using the multilateration system. The TDOA measurement sets obtained with each of the deployed GRS as reference are used in solving a derived TDOA based residual equation. The GRS with the least TDOA measurement residual is chosen as reference for subsequent tracking of the aircraft. Another approach to improve the PE accuracy of the lateration algorithm is using multiple GRSs as reference to generate the TDOA measurement set [9,11]. Using either single or multiple GRSs as reference to generate the TDOA measurement set, there is need to select the suitable reference GRS for the estimation. This is because the choice of the reference GRS to generate the TDOA measurement set for the lateration algorithm depends on the location of the aircraft relative to the geometry of the GRS configuration [12, 14]. In this work, with a total of five deployed GRSs and using a pair of GRS as reference for the TDOA measurement set generation, a technique based on condition number calculation for selecting the suitable GRS reference pair for the lateration algorithm is proposed. The technique involves selecting the GRS pair whose TDOA measurement set resulted in the least condition number of a derived matrix as the reference. The suggested technique is validated using 5-square and pentagon GRS configurations.

The remainder of the paper is organized as follows: Section II describes the two-reference PE closed-form lateration algorithm and the condition number analysis, while in Section III, the path difference (PD) measurement (TDOA measurement distance equivalent) based GRS reference pair selection technique is presented. The simulation result and discussion are presented in Section IV, which is followed by conclusion in Section V.

II. METHODOLOGY

This section of the paper gives a detail derivation of the two-reference PE closed-form lateration algorithm which is followed by the effect of the PD estimation (PDE) error (TDOA estimation error distance equivalent) on the PE accuracy of the lateration algorithm.

A. Two-reference PE Closed-form Lateration Algorithm

Let an aircraft located at $\mathbf{x_e} = (x, y, z)$ transmit a signal that is detected by the *i*-th GRS with coordinate $\mathbf{S}_i = (x_i, y_i, z_i)$. The propagation time of the signal from the aircraft to the *i*-th GRS is denoted as τ_i. The distance travelled by the signal from aircraft to the *i*-th GRS is calculated as:

$$\begin{aligned} d_i &= c \times \tau_i \\ &= \sqrt{(x - x_i)^2 + (y - y_i)^2 + (z - z_i)^2} \end{aligned} \tag{1}$$

where: $c = 3 \times 10^8$ m/s

To differentiate between reference and non-reference GRSs, let the GRSs labeled *i*-th and *j*-th with coordinate $\mathbf{S}_j = (x_j, y_j, z_j)$ be chosen as the reference GRS pair for the TDOA estimation and the GRS labelled *m*-th with coordinate $\mathbf{S}_m = (x_m, y_m, z_m)$ be the non-reference GRS. Two PD measurement equations are obtained and expressed as follow:

$$d_{im} = d_i - d_m \tag{2a}$$

$$d_{jm} = d_j - d_m \tag{2b}$$

Further simplification of Eq. (2a) and Eq. (2b) will result in Eq. (3a) and Eq. (3b) respectively.

$$\frac{d_{im}}{2} + \frac{(d_m)^2 + (d_i)^2}{2d_{im}} = -d_m \tag{3a}$$

$$\frac{d_{jm}}{2} + \frac{(d_m)^2 + (d_j)^2}{2d_{jm}} = -d_m \tag{3b}$$

The detailed derivations from Eq. (2) to Eq. (3) can be found in [16]. Equate Eq. (3a) and Eq. (3b) to eliminate $-d_m$ as shown in Eq. (4):

$$\frac{d_{im}}{2} + \frac{(d_m)^2 + (d_i)^2}{2d_{im}} = \frac{d_{jm}}{2} + \frac{(d_m)^2 + (d_j)^2}{2d_{jm}} \tag{4}$$

Eq. (4) is further simplified and expressed as a function of the aircraft position and GRS coordinates as indicated in Eq. (5).

$$\begin{aligned} x\left(\frac{X_{im}}{d_{im}} - \frac{X_{jm}}{d_{jm}}\right) + y\left(\frac{Y_{im}}{d_{im}} - \frac{Y_{jm}}{d_{jm}}\right) \\ + z\left(\frac{Z_{im}}{d_{im}} - \frac{Z_{jm}}{d_{jm}}\right) = \frac{d_{jm} - d_{im}}{2} + \\ \frac{K_{mj}}{2d_{mj}} + \frac{K_{mi}}{2d_{mi}} \end{aligned} \tag{5}$$

where:

$$X_{im} = x_i - x_m$$

$$X_{jm} = x_j - x_m$$

$$Y_{im} = y_i - y_m$$

$$Y_{jm} = y_j - y_m$$

$$Z_{im} = z_i - z_m$$

$$Z_{jm} = z_j - z_m$$

$$K_{mi} = (x_m^2 + y_m^2 + z_m^2) - (x_i^2 + y_i^2 + z_i^2)$$

$$K_{mj} = (x_m^2 + y_m^2 + z_m^2) - (x_j^2 + y_j^2 + z_j^2)$$

Eq. (5) is the 3-D hyperbolic equation obtained using the GRSs labelled *i*-th and *j*-th as the reference pair and the *m*-th GRS as non-reference. Let a total of $N = 5$ GRSs be deployed. With a GRS pair as reference for the TDOA estimation, the total number of non-reference GRSs are three resulting in three hyperbolic plane equations in the form of Eq. (5). Let the two remaining non-reference GRSs be labelled *n*-th and *p*-th with coordinates $\mathbf{S}_n = (x_n, y_n, z_n)$ and $\mathbf{S}_p = (x_p, y_p, z_p)$ respectively, then, their resulting hyperbolic equations with *i*-th and *j*-th as GRS reference pair are:

$$\begin{aligned} x\left(\frac{X_{in}}{d_{in}} - \frac{X_{jn}}{d_{jn}}\right) + y\left(\frac{Y_{in}}{d_{in}} - \frac{Y_{jn}}{d_{jn}}\right) \\ + z\left(\frac{Z_{in}}{d_{in}} - \frac{Z_{jn}}{d_{jn}}\right) = \frac{d_{jn} - d_{in}}{2} + \\ \frac{K_{nj}}{2d_{nj}} + \frac{K_{ni}}{2d_{ni}} \end{aligned} \tag{6}$$

$$x\left(\frac{X_{ip}}{d_{ip}}-\frac{X_{jp}}{d_{jp}}\right)+\ y\left(\frac{Y_{ip}}{d_{ip}}-\frac{Y_{jp}}{d_{jp}}\right)+ z\left(\frac{Z_{ip}}{d_{ip}}-\frac{Z_{jp}}{d_{jp}}\right)=\frac{d_{jp}-d_{ip}}{2}+\frac{K_{pj}}{2d_{pj}}+\frac{K_{pi}}{2d_{pi}} \tag{7}$$

Eq. (5), Eq. (6) and Eq. (7) presented in a matrix form is as follows:

$$\mathbf{A}_{ij}\mathbf{x}_e=\mathbf{b}_{ij} \tag{8}$$

where:

$$\mathbf{x}_e=[x,y,\mathrm{z}]^T$$

$$\mathbf{b}_{ij}=\begin{bmatrix}\dfrac{d_{jm}-d_{im}}{2}+\dfrac{K_{mj}}{2d_{mj}}+\dfrac{K_{mi}}{2d_{mi}}\\ \dfrac{d_{jn}-d_{in}}{2}+\dfrac{K_{nj}}{2d_{nj}}+\dfrac{K_{ni}}{2d_{ni}}\\ \dfrac{d_{jp}-d_{ip}}{2}+\dfrac{K_{pj}}{2d_{pj}}+\dfrac{K_{pi}}{2d_{pi}}\end{bmatrix}$$

$$\mathbf{A}_{ij}=\begin{bmatrix}\left(\dfrac{X_{im}}{d_{im}}-\dfrac{X_{jm}}{d_{jm}}\right) & \left(\dfrac{Y_{im}}{d_{im}}-\dfrac{Y_{jm}}{d_{jm}}\right) & \left(\dfrac{Z_{im}}{d_{im}}-\dfrac{Z_{jm}}{d_{jm}}\right)\\ \left(\dfrac{X_{in}}{d_{in}}-\dfrac{X_{jn}}{d_{jn}}\right) & \left(\dfrac{Y_{in}}{d_{in}}-\dfrac{Y_{jn}}{d_{jn}}\right) & \left(\dfrac{Z_{in}}{d_{in}}-\dfrac{Z_{jn}}{d_{jn}}\right)\\ \left(\dfrac{X_{ip}}{d_{ip}}-\dfrac{X_{jp}}{d_{jp}}\right) & \left(\dfrac{Z_{ip}}{d_{ip}}-\dfrac{Z_{jp}}{d_{jp}}\right) & \left(\dfrac{Y_{ip}}{d_{ip}}-\dfrac{Y_{jp}}{d_{jp}}\right)\end{bmatrix}$$

The Matrix in Eq. (8) is the PE mathematical model for a multilateration system based on 5 GRSs. It represents the least square (LS) problem with the aircraft position as the unknown. The aircraft position is obtained given the TDOA measurement set by solving the LS problem using Eq. (9).

$$\mathbf{x}_e=\left(\mathbf{A}_{ij}\right)^{-1}\mathbf{b} \tag{9}$$

In the next section, the effect of error in the input variable on the overall PE accuracy of the lateration algorithm is determined through matrix condition number calculation.

B. Effect of PD Measurement Error on the Lateration Algorithm PE accuracy

In practical application, the PD measurements that is d_{im} and d_{jm} in Eq. (2) contains an error which subsequently affects the solution obtained using Eq. (9). The effect of the error on the solution of Eq. (9) depends on the condition number of matrix $\mathbf{A}_{ij}$ denoted as $K(\mathbf{A}_{ij})$ [17].

Mathematically, $K(\mathbf{A}_{ij})$is expressed as follows:

$$K(\mathbf{A}_{ij})=\left\|\mathbf{A}_{ij}\right\|_2\times\left\|\left(\mathbf{A}_{ij}\right)^{-1}\right\|_2 \tag{10}$$

where:

$$\left\|\mathbf{A}_{ij}\right\|_2=\sqrt{\begin{array}{l}\left|B_{i,j,m}\right|^2+\left|C_{i,j,m}\right|^2+\left|D_{i,j,m}\right|^2+\\ \left|B_{i,j,n}\right|^2+\left|C_{i,j,n}\right|^2+\left|D_{i,j,n}\right|^2+\\ \left|B_{i,j,p}\right|^2+\left|C_{i,j,p}\right|^2+\left|D_{i,j,p}\right|^2\end{array}} \tag{11a}$$

$$\left\|\left(\mathbf{A}_{ij}\right)^{-1}\right\|_2=\frac{1}{\det(\mathbf{A}_{ij})}\sqrt{\begin{array}{l}\left|B_{i,j,m}\right|^2+\left|C_{i,j,m}\right|^2+\left|D_{i,j,m}\right|^2+\\ \left|B_{i,j,n}\right|^2+\left|C_{i,j,n}\right|^2+\left|D_{i,j,n}\right|^2+\\ \left|B_{i,j,p}\right|^2+\left|C_{i,j,p}\right|^2+\left|D_{i,j,p}\right|^2\end{array}} \tag{11b}$$

$$\begin{aligned}\det(\mathbf{A}_{ij})=&\left(B_{i,j,m}\times C_{i,j,n}\times D_{i,j,p}\right)-\left(B_{i,j,m}\times C_{i,j,p}\times D_{i,j,n}\right)-\\ &\left(B_{i,j,n}\times C_{i,j,m}\times D_{i,j,p}\right)+\left(B_{i,j,p}\times C_{i,j,m}\times D_{i,j,n}\right)+\\ &\left(B_{i,j,n}\times C_{i,j,p}\times D_{i,j,m}\right)-\left(B_{i,j,p}\times C_{i,j,n}\times D_{i,j,m}\right)\end{aligned} \tag{11c}$$

See Appendix A for coefficients of Eq. (11). The higher the $K(\mathbf{A}_{ij})$ value, the higher the error in the solution of Eq. (9) which is due to the PDE error. Different GRS reference pairs will result in different TDOA measurement sets which subsequently leads to different entries of matrix $\mathbf{A}_{ij}$. This results in different values of $K(\mathbf{A}_{ij})$. With $N=5$ GRSs out of which a pair of GRS is used as reference for the TDOA measurement set generation, the total number of possible GRS reference pair combinations are 10. Table 1 shows the different combinations of the GRS reference pair.

Table 1
All possible combinations of GRS pair for TDOA measurement set generation

	GRS reference pair combination	
	i-th	j-th
Pair 1	GRS 1	GRS 2
Pair 2	GRS 1	GRS 3
Pair 3	GRS 1	GRS 4
Pair 4	GRS 1	GRS 5
Pair 5	GRS 2	GRS 3
Pair 6	GRS 2	GRS 4
Pair 7	GRS 2	GRS 5
Pair 8	GRS 3	GRS 4
Pair 9	GRS 3	GRS 5
Pair 10	GRS 4	GRS 5

Let the distribution of the five GRSs be in a 5-square configuration as shown in Figure 1.

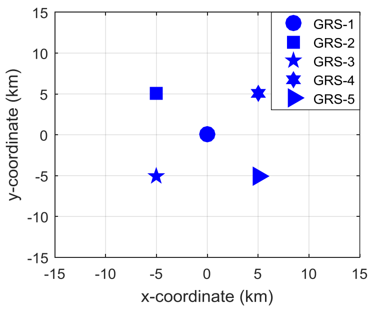

Figure 1: The distribution of GRS in a five-square configuration [10 km separation]

Consider three aircraft positions:

$$\mathbf{x}_{e,a} = (5\ km, 50\ km, 1\ km)$$
$$\mathbf{x}_{e,b} = (-50\ km, 5\ km, 7\ km)$$
$$\mathbf{x}_{e,c} = (50\ km, -50\ km, 7\ km)$$

For each of the aircraft positions, the TDOA measurement set using all the possible GRS reference pair combinations as defined in Table 1 are obtained and substituted in matrix $\mathbf{A}_{ij}$ in Eq. (8). The condition number of each of the matrix is calculated using Eq. (10) and is shown in Table 2.

Table 2
The $K(\mathbf{A}_{ij})$ value for all the GRS pair with the GRSs in 5-square configuration. Red shade indicates the pair with the highest $K(\mathbf{A}_{ij})$ value and yellow shade indicates the pair with the least $K(\mathbf{A}_{ij})$ value.

No.	GRS reference pair	Aircraft position		
		$\mathbf{x}_{e,a}$	$\mathbf{x}_{e,b}$	$\mathbf{x}_{e,c}$
1	Pair 1	951	725	2017
2	Pair 2	1036	634	3×10^6
3	Pair 3	1033	634	3×10^6
4	Pair 4	931	693	2214
5	Pair 5	1036	654	3×10^6
6	Pair 6	1036	654	3×10^6
7	Pair 7	1036	654	3×10^6
8	Pair 8	275	164	3×10^6
9	Pair 9	275	164	3×10^6
10	Pair 10	275	164	3×10^6

From Table 2, it is seen that $K(\mathbf{A}_{ij})$ varies with the GRS reference pair and aircraft position. At aircraft position $\mathbf{x}_{e,a}$, GRS reference pairs 8, 9 and 10 have the least $K(\mathbf{A}_{ij})$ value of about 275 while GRS reference pairs 2, 5, 6, and 7 have the highest $K(\mathbf{A}_{ij})$ value of about 1036. This means that the TDOA measurement sets obtained with GRS reference pairs 8, 9, and 10 are the most suitable for use with the lateration algorithm to estimate the aircraft located at $\mathbf{x}_{e,a} = (5\ km, 50\ km, 1\ km)$. The TDOA measurement sets of these GRS reference pairs used with the lateration algorithm will result in aircraft position estimates with minimum error.

Extending the analysis to aircrafts at positions $\mathbf{x}_{e,b}$ and $\mathbf{x}_{e,c}$, GRS reference pairs 8, 9 and 10 are the most suitable pairs to be used as references in generating the TDOA measurement set for the PE of the aircraft at $\mathbf{x}_{e,b}$, while GRS reference pair 1 is the most suitable to estimate the position of the aircraft at $\mathbf{x}_{e,c}$. Thus, there is need to choose the suitable GRS pair to use as reference in generating the TDOA measurement set for the PE of an aircraft at any given position. This is to improve the accuracy at which aircraft positions are estimated. Matrix $\mathbf{A}_{ij}$ in Eq. (8) is a function of the PD measurements and GRS coordinates. It cannot be used for selecting the suitable GRS reference pair. This is because the GRS reference pair selection process is performed prior to the actual PE process and at that stage, only the PD measurements are available. Hence, there is need to determine the GRS reference pair to be used in obtaining the PD measurement set independent of the GRS coordinates.

In the next section, a technique for selecting the suitable GRS reference pair based on only generated PD measurement set is presented.

III. Reference Station Selection Based on PD Measurement Set

The technique to determine the GRS reference pair to be used in generating the suitable PD measurement sets is described in this section. The matrix $\mathbf{A}_{ij}$ in Eq. (8) is a function of both the PD measurement and GRS coordinates. It can be factorized into two matrices with one having only the PD measurement set obtained using any of the GRS reference pair combinations presented in Table 1 as it entries. The factorization of matrix $\mathbf{A}_{ij}$ is as follows:

$$\mathbf{A}_{ij} = \begin{bmatrix} \left(\frac{X_{im}}{d_{im}} - \frac{X_{jm}}{d_{jm}}\right) & \left(\frac{Y_{im}}{d_{im}} - \frac{Y_{jm}}{d_{jm}}\right) & \left(\frac{Z_{im}}{d_{im}} - \frac{Z_{jm}}{d_{jm}}\right) \\ \left(\frac{X_{in}}{d_{in}} - \frac{X_{jn}}{d_{jn}}\right) & \left(\frac{Y_{in}}{d_{in}} - \frac{Y_{jn}}{d_{jn}}\right) & \left(\frac{Z_{in}}{d_{in}} - \frac{Z_{jn}}{d_{jn}}\right) \\ \left(\frac{X_{ip}}{d_{ip}} - \frac{X_{jp}}{d_{jp}}\right) & \left(\frac{Z_{ip}}{d_{ip}} - \frac{Z_{jp}}{d_{jp}}\right) & \left(\frac{Y_{ip}}{d_{ip}} - \frac{Y_{jp}}{d_{jp}}\right) \end{bmatrix} \tag{12a}$$

$$= \begin{bmatrix} \left(\frac{d_{jm}X_{im} - d_{im}X_{jm}}{d_{jm}d_{im}}\right) & \left(\frac{d_{jm}Y_{im} - d_{im}Y_{jm}}{d_{jm}d_{im}}\right) & \left(\frac{d_{jm}Z_{im} - d_{im}Z_{jm}}{d_{jm}d_{im}}\right) \\ \left(\frac{d_{jn}X_{in} - d_{in}X_{jn}}{d_{jn}d_{in}}\right) & \left(\frac{d_{jn}Y_{in} - d_{in}Y_{jn}}{d_{jn}d_{in}}\right) & \left(\frac{d_{jn}Z_{in} - d_{in}Z_{jn}}{d_{jn}d_{in}}\right) \\ \left(\frac{d_{jp}X_{ip} - d_{ip}X_{jp}}{d_{jp}d_{ip}}\right) & \left(\frac{d_{jp}Y_{ip} - d_{ip}Y_{jp}}{d_{jp}d_{ip}}\right) & \left(\frac{d_{jp}Z_{ip} - d_{ip}Z_{jp}}{d_{jp}d_{ip}}\right) \end{bmatrix} \tag{12b}$$

$$= \begin{bmatrix} \left(d_{jm}d_{im}\right)^{-1} & 0 & 0 \\ & \left(d_{jn}d_{in}\right)^{-1} & \\ & & \left(d_{jp}d_{ip}\right)^{-1} \end{bmatrix} \times \begin{bmatrix} \left(d_{jm}X_{im} - d_{im}X_{jm}\right) & \left(d_{jm}Y_{im} - d_{im}Y_{jm}\right) & \left(d_{jm}Z_{im} - d_{im}Z_{jm}\right) \\ \left(d_{jn}X_{in} - d_{in}X_{jn}\right) & \left(d_{jn}Y_{in} - d_{in}Y_{jn}\right) & \left(d_{jn}Z_{in} - d_{in}Z_{jn}\right) \\ \left(d_{jp}X_{ip} - d_{ip}X_{jp}\right) & \left(d_{jp}Y_{ip} - d_{ip}Y_{jp}\right) & \left(d_{jp}Z_{ip} - d_{ip}Z_{jp}\right) \end{bmatrix} \tag{12c}$$

From Eq. (12c), Let

$$\mathbf{M}_{ij}=\begin{bmatrix}\left(d_{jm}d_{im}\right)^{-1} & 0 & 0\\ 0 & \left(d_{jn}d_{in}\right)^{-1} & 0\\ 0 & 0 & \left(d_{jp}d_{ip}\right)^{-1}\end{bmatrix} \tag{13}$$

and

$$\mathbf{N}_{ij}=\begin{bmatrix}\left(d_{jm}X_{im}-d_{im}X_{jm}\right) & \left(d_{jm}Y_{im}-d_{im}Y_{jm}\right) & \left(d_{jm}Z_{im}-d_{im}Z_{jm}\right)\\ \left(d_{jn}X_{in}-d_{in}X_{jn}\right) & \left(d_{jn}Y_{in}-d_{in}Y_{jn}\right) & \left(d_{jn}Z_{in}-d_{in}Z_{jn}\right)\\ \left(d_{jp}X_{ip}-d_{ip}X_{jp}\right) & \left(d_{jp}Y_{ip}-d_{ip}Y_{jp}\right) & \left(d_{jp}Z_{ip}-d_{ip}Z_{jp}\right)\end{bmatrix} \tag{14}$$

The matrix $\mathbf{M}_{ij}$ in Eq. (13) is seen to be a function of only the PD measurements. It is possible to determine the suitable GRS pair as reference for the lateration algorithm by looking at its condition number. The condition number of matrix $\mathbf{M}_{ij}$, denoted as $K(\mathbf{M}_{ij})$ is obtained as follows:

$$K(\mathbf{M}_{ij})=\left(\frac{d_{jn}\times d_{in}\times d_{jp}\times d_{ip}}{d_{im}\times d_{jn}}\right)+\left(\frac{d_{jm}\times d_{im}\times d_{jp}\times d_{ip}}{d_{in}\times d_{jn}}\right)+\left(\frac{d_{jn}\times d_{in}\times d_{jm}\times d_{im}}{d_{ip}\times d_{jp}}\right) \tag{15}$$

The use of $K(\mathbf{M}_{ij})$ in Eq. (15) to determine the GRS pair that is suitable as reference for generating the PD measurement set to be used in the PE with lateration is considered in the next section.

IV. Result and Discussion

In this section, the use of $K(\mathbf{M}_{ij})$ in Eq. (15) for selecting the suitable GRS pair as reference is validated by comparing with $K(\mathbf{A}_{ij})$ in Eq. (10). The validation is carried out at the selected aircraft positions defined in Table 3.

Table 3
Selected aircraft positions for validation of the proposed technique.

No.	Aircraft position	Emitter coordinates x (km)	y (km)	z (km)
1	A	5	-50	1
2	B	-20	20	4
3	C	100	50	7
4	D	-50	-50	15

The GRS configurations considered are the 5-squared GRS configuration shown in Figure 1 and pentagon configuration shown in Figure 2.

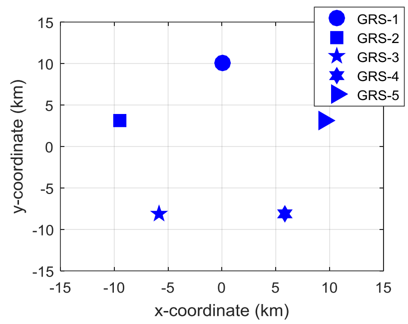

Figure 2: The distribution of the GRS in pentagon configuration

For each of the GRS configurations, $K(\mathbf{A}_{ij})$ from Eq. (10) and $K(\mathbf{M}_{ij})$ from Eq. (15) for each GRS pair presented in Table 1 are obtained and compared. Table 4 and Table 5 show the comparison between $K(\mathbf{A}_{ij})$ and $K(\mathbf{M}_{ij})$ for the 5-square and pentagon GRS configurations, respectively. For both GRS configurations and aircraft positions considered, the pair with the least $K(\mathbf{A}_{ij})$ value also has the least $K(\mathbf{M}_{ij})$ value. For instance, from Table 1 and at aircraft position B, GRS reference pair 1 has the least condition number value which is $K(\mathbf{A}_{ij}) = 766$ and also has the least $K(\mathbf{M}_{ij}) = 14$. This means that the suitable GRS pair as reference to generate the PD measurement set for the PE of an aircraft at position B is GRS pair 1.

It can also be seen that some aircraft positions have more than one GRS reference pair combinations having the least $K(\mathbf{A}_{ij})$ and $K(\mathbf{M}_{ij})$ values. For instance, in Table 4 which shows the condition number comparison for the 5-square configuration, aircraft positions A, C, and D all have three GRS reference pair combinations with equal $K(\mathbf{A}_{ij})$ value. These GRS reference pairs happened to also have the least $K(\mathbf{A}_{ij})$ values which are GRS reference pairs 8, 9 and 10. The $K(\mathbf{A}_{ij})$ value for these three GRS reference pair combinations at aircraft positions A, C and D are 176, 778 and 1156 respectively while the $K(\mathbf{M}_{ij})$ value for these three GRS reference pair combinations are also the least among all the pairs with values of 2, 1 and 1 for aircraft at aircraft positions A, C and D respectively. Thus, it is seen that even though some aircraft positions have more than one GRS reference pair combinations that leads to better PE accuracy, the suggested techniques based on Eq. (15) can identify all these GRS reference pair combinations to be used in generating the PD measurement set for the lateration algorithm.

Extending the analysis to Table 5 which present the condition number comparison for the pentagon GRS configuration, it is seen that the same conclusion can be deduced. All the selected aircraft positions each have four GRS reference pair combinations with equal $K(\mathbf{A}_{ij})$ values. These values are 873, 421, 371, and 176 for aircraft at positions A, B, C and D respectively. The corresponding $K(\mathbf{M}_{ij})$ values for these aircraft positions with the least $K(\mathbf{A}_{ij})$ values are 3, 14, 6 and 2 respectively which also happened to be the GRS reference pair combinations having the least values. It should be note that the higher the $K(\mathbf{A}_{ij})$ or $K(\mathbf{M}_{ij})$ values, the higher the PE error. This means that the best GRS pair can be selected for every aircraft position but the value of error differs. Some aircraft positions will

Table 4
$K(\mathbf{A}_{ij})$ and $K(\mathbf{M}_{ij})$ values comparison for the 5-square GRS configuration. Yellow shade indicates the GRS pair with the least $K(\mathbf{A}_{ij})$ value while green shade indicates the GRS pair with the least $K(\mathbf{M}_{ij})$ value.

No.	GRS pair	Aircraft Position							
		A		B		C		D	
		$K(\mathbf{A}_{ij})$	$K(\mathbf{M}_{ij})$	$K(\mathbf{A}_{ij})$	$K(\mathbf{M}_{ij})$	$K(\mathbf{A}_{ij})$	$K(\mathbf{M}_{ij})$	$K(\mathbf{A}_{ij})$	$K(\mathbf{M}_{ij})$
1	Pair 1	701	13	766	14	2120	5	2.1×10^7	1.3×10^4
2	Pair 2	638	10	9.2×10^5	9916	2647	9	2.2×10^4	37
3	Pair 3	643	11	9.2×10^5	9835	2647	10	2.2×10^4	40
4	Pair 4	708	14	965	18	1929	7	1.5×10^7	1.4×10^4
5	Pair 5	638	9	9.2×10^5	9916	2647	9	2.2×10^4	37
6	Pair 6	638	9	9.2×10^5	9916	2647	9	2.2×10^4	37
7	Pair 7	638	9	9.2×10^5	9916	2647	9	2.2×10^4	37
8	Pair 8	176	2	10.1×10^5	82	778	1	1156	1
9	Pair 9	176	2	10.1×10^5	82	778	1	1156	1
10	Pair 10	176	2	10.1×10^5	82	778	1	1156	1

Table 5
$K(\mathbf{A}_{ij})$ and $K(\mathbf{M}_{ij})$ comparison for the pentagon GRS configuration. Yellow shade indicates the GRS pair with the least $K(\mathbf{A}_{ij})$ value while green shade indicates the GRS pair with the least $K(\mathbf{M}_{ij})$ value.

No.	GRS pair	Aircraft Position							
		A		B		C		D	
		$K(\mathbf{A}_{ij})$	$K(\mathbf{M}_{ij})$	$K(\mathbf{A}_{ij})$	$K(\mathbf{M}_{ij})$	$K(\mathbf{A}_{ij})$	$K(\mathbf{M}_{ij})$	$K(\mathbf{A}_{ij})$	$K(\mathbf{M}_{ij})$
1	Pair 1	1.5e4	20	1141	5	404	5	191	5
2	Pair 2	873	3	421	14	371	6	176	2
3	Pair 3	958	4	226	7	2658	9	386	9
4	Pair 4	1.3e4	23	208	3	3761	10	1019	4
5	Pair 5	873	3	421	14	371	6	176	2
6	Pair 6	873	3	421	14	371	6	176	2
7	Pair 7	873	3	421	14	371	6	176	2
8	Pair 8	5068	6	1066	8	769	12	1198	10
9	Pair 9	5068	6	1066	8	769	12	1198	10
10	Pair 10	5068	6	1066	8	769	12	1198	10

have higher PE error values that others. In the end, the least PE errors are obtained for each aircraft position using the suggested technique.

Based on the results presented in Tables 4 and Table 5, it is possible to determine the suitable GRS pair as reference to generate the PD measurement set for PE using matrix $\mathbf{M}_{ij}$ in Eq. (13). This is done by calculating the $K(\mathbf{M}_{ij})$ value using Eq. (15) for all the possible GRS pair combinations and then choose the GRS pair with the least condition number as the reference.

V. Conclusion

A technique for selecting the suitable GRS pair as reference to generate the PD measurement set to be used in PE with the closed-form lateration algorithm is suggested in this paper. This is done to improve the PE accuracy of the lateration algorithm. The suggested technique involves calculating the condition number of a matrix with PD measurements as the only entries. The condition number for all possible GRS pairs as reference are obtained and the pair with the least condition number is chosen as the reference. Using 5-square and pentagon GRS configurations, the technique was validated at some selected aircraft positions. The result verified that the technique can be used in selecting the suitable GRS reference pair. This work only focuses on using PD measurements to select the suitable GRS reference pair for PE. The actual improvement in the PE accuracy of the lateration algorithm depends on the PD measurement error which is related to the TDOA estimation algorithm used. Further research should focus on determining the percentage improvement in the PE accuracy of the lateration algorithm with the proposed reference selection technique.

APPENDIX

Coefficients of Eq. (11):

$$B_{i,j,m} = \left(\frac{X_{im}}{d_{im}} - \frac{X_{jm}}{d_{jm}}\right) \qquad C_{i,j,m} = \left(\frac{Y_{im}}{d_{im}} - \frac{Y_{jm}}{d_{jm}}\right)$$

$$D_{i,j,m} = \left(\frac{Z_{im}}{d_{im}} - \frac{Z_{jm}}{d_{jm}}\right) \qquad B_{i,j,n} = \left(\frac{X_{in}}{d_{in}} - \frac{X_{jn}}{d_{jn}}\right)$$

$$C_{i,j,n} = \left(\frac{Y_{in}}{d_{in}} - \frac{Y_{jn}}{d_{jn}}\right) \qquad D_{i,j,n} = \left(\frac{Z_{in}}{d_{in}} - \frac{Z_{jn}}{d_{jn}}\right)$$

$$B_{i,j,p} = \left(\frac{X_{ip}}{d_{ip}} - \frac{X_{jp}}{d_{jp}}\right) \qquad C_{i,j,p} = \left(\frac{Z_{ip}}{d_{ip}} - \frac{Z_{jp}}{d_{jp}}\right)$$

$$D_{i,j,p} = \left(\frac{Y_{ip}}{d_{ip}} - \frac{Y_{jp}}{d_{jp}}\right)$$

ACKNOWLEDGMENT

The authors thank Universiti Teknologi Malaysia (UTM) for providing the resources and support for this research.

REFERENCES

[1] M. A. C. Duran *et al.*, “Terrestrial Network-Based Positioning and Navigation,” in *Satellite and Terrestrial Radio Positioning Techniques*, 2012, pp. 75–153.

[2] W. H. L. Neven, T. J. Quilter, R. Weedo, and R. A. Hogendoorn, “Wide area multilateration (WAM),” Eurocontrol, Report on EATMP TRS 131/04 Version 1.1, 2005.

[3] A. S. Yaro and A. Z. Sha’meri, “Mathematical Model of Position Estimation Error for a Multiangulation System,” in *the 6th International Graduate Conference on Engineering, Science & Humanity: Empowering innovation and Entrepreneurship for sustainable Development*, 2016, pp. 134–136.

[4] L. Rui and K. C. Ho, “Bias analysis of maximum likelihood target location estimator,” *IEEE Transactions on Aerospace and Electronic Systems*, vol. 50, no. 4, pp. 2679–2693, Oct. 2014.

[5] G. Galati, M. Leonardi, J. V. Balbastre-Tejedor, and I. I. A. Mantilla-Gaviria, “Time-difference-of-arrival regularised location estimator for multilateration systems,” *IET Radar, Sonar & Navigation*, vol. 8, no. 5, pp. 479–489, Jun. 2014.

[6] D. E. Chaitanya, M. N. V. S. S. Kumar, G. S. Rao, and R. Goswami, “Convergence issues of taylor series method in determining unknown target location using hyperbolic multilateration,” *2014 International Conference on Science Engineering and Management Research, ICSEMR 2014*, no. 1, pp. 1–4, 2015.

[7] W. Lei and B. Chen, “High-precision hyperboloid location method using passive time-difference-of-arrival measurements,” *IET Radar, Sonar & Navigation*, vol. 7, no. 6, pp. 710–717, 2013.

[8] A. Z. Sha’ameri, Y. A. Shehu, and W. Asuti, “Performance analysis of a minimum configuration multilateration system for airborne emitter position estimation,” *Defence S and T Technical Bulletin*, vol. 8, no. 1, pp. 27–41, 2015.

[9] H. Torbati Fard, M. Atashbar, Y. Norouzi, and F. Hojjat Kaskani, “Multireference TDOA-based source localization,” *Turkish Journal of Electrical Engineering & Computer Sciences*, vol. 21, pp. 1920–1929, 2013.

[10] M. Malanowski and K. Kulpa, “Two methods for target localization in multistatic passive radar,” *IEEE Transactions on Aerospace and Electronic Systems*, vol. 48, no. 1, pp. 572–580, Jan. 2012.

[11] M. D. Gillette and H. F. Silverman, “A linear closed-form algorithm for source localization from time-differences of arrival,” *IEEE Signal Processing Letters*, vol. 15, no. 1, pp. 1–4, 2008.

[12] Q. Xu, Y. Lei, J. Cao, and H. Wei, “An improved algorithm based on reference selection for time difference of arrival location,” *Proceedings - 2014 7th International Congress on Image and Signal Processing, CISP 2014*, no. 3, pp. 953–957, 2014.

[13] K. C. Ho, “Bias reduction for an explicit solution of source localization using TDOA,” *IEEE Transactions on Signal Processing*, vol. 60, no. 5, pp. 2101–2114, 2012.

[14] J. Zhou, J. Shi, and X. Qu, “Landmark placement for wireless localization in rectangular-shaped industrial facilities,” *IEEE Transactions on Vehicular Technology*, vol. 59, no. 6, pp. 3081–3090, 2010.

[15] Y. Chen, J. A. Francisco, W. Trappe, and R. P. Martin, “A Practical Approach to Landmark Deployment for Indoor Localization,” in *2006 3rd Annual IEEE Communications Society on Sensor and Ad Hoc Communications and Networks*, 2006, vol. 1, pp. 365–373.

[16] R. Bucher and D. Misra, “A Synthesizable VHDL Model of the Exact Solution for Three-dimensional Hyperbolic Positioning System,” *VLSI Design*, vol. 15, no. 2, pp. 507–520, 2002.

[17] G. H. Golub and C. F. Van Loan, *Matrix Computations*, 4th ed. Johns Hopkins University Press, 2013.